# AN INVESTIGATION OF ABS STRATEGIES FOR ARTICULATED VEHICLES

**F.W. Kienhöfer and D. Cebon**

Cambridge University, Engineering Department
CB2 1PZ, United Kingdom.

## ABSTRACT

This paper investigates anti-lock braking control strategies for heavy goods vehicles. A mathematical model of the braking of an experimental articulated vehicle is developed. The model includes the details of vehicle dynamics, the ABS control algorithm as well as the mechanics of the foundation brakes and the pneumatic and mechanical systems. Parameters for the model are determined from tests on an instrumented experimental tractor semi-trailer. The model is validated by comparing its performance to experimental results for the instrumented vehicle undergoing straight-line braking tests on several test track surfaces. The simulation and experimental results show good agreement. The model is used to evaluate the benefits of wheel-slip control. The results indicate that wheel-slip control has the potential to reduce braking distances by approximately 25%, however some hardware modifications may be needed to achieve this.

## INTRODUCTION

The braking system is a critical safety component of a vehicle. ABS systems are mandatory on European heavy vehicles. This paper considers the performance of ABS system and whether improvements could be made to stopping performance.

In early computer simulations, Fancher showed that the steering axles play an important part in the braking of articulated vehicles (Fancher 1976). He later compared a 'worst-wheel' ABS strategy to an independent wheel strategy (Fancher 1985) and showed that lightly loaded vehicles can jack-knife in braking-in-a-turn manoeuvres nearing the limits of tyre-road adhesion, when independent wheel control is used on a tractor's rear wheels. These simulations were later extended to include driver models in a closed loop system (MacAdam 1985). The conclusions were that the rear axle of a tractor should be equipped with a worst-wheel' strategy to assist drivers to maintain path control, and an independent wheel control strategy should be implemented on steering axles so as to improve the deceleration performance.

Van Zanten (Zanten 2002) discussed the extension of ABS - which controls individual wheel behaviour - to ESP (Electronic Stability Program) – which controls the whole vehicle. A combination of sensor measurements and estimation algorithms, using model-matching control can be used to prove feedback signals. The adaptation of these intelligent systems from passenger cars to commercial vehicles, as well as systems designed originally for commercial vehicles, was discussed by Palkovics and Fries (Palkovics 2001). Commercially available systems, incorporating anti-jack-knifing and stability enhancement systems, include the Haldex EB+ and the Knorr-Bremse ROP (Roll Over Protection).

Conventional air-actuated ABS systems for heavy vehicles use a 'bang-bang' control approach to controlling wheel rotation under braking. There appears to be some scope for alternative strategies.

McLoughlin (McLoughlin 1985) analysed wheel-slip control as an alternative to conventional ABS strategies, and concluded that wheel-slip control offers advantages for a range of tyre friction characteristics. Wheel-slip control seeks to continually optimise the slip during braking to generate maximum deceleration. Hardy and Cebon (Hardy 1995) used a validated ABS simulation model to show that wheel-slip control can improve the stopping distance of heavy trucks fitted with either steel or air suspension on rough roads. The benefits are particularly pronounced when the road surface roughness increases.

Implementation of wheel-slip control however is not straightforward due to limitations caused by pneumatic time delays and the difficulty in measuring absolute vehicle speed under braking. These problems were discussed by Gissinger et al (Gissinger 2003), who concluded that a complete redesign of brake actuation and hardware was required to implement wheel-slip control.

A number of researchers have investigated wheel-slip control for passenger cars as well as heavy commercial vehicles. Kimbrough (Kimbrough 1994; Kimbrough 1999) combined a simple bilinear tyre model with a Lyapunov Stability Criterion so as to develop a method to account for tyre saturation. The inherent robustness of Fuzzy Logic control has made the strategy a frequent choice in developing advanced wheel-slip control algorithms (Akey 1995; Akey 1996; Chen 2000; Will 2000; Yu 2002). Jun (Jun 1998) has presented a comparison of conventional threshold ABS, fuzzy logic, sliding mode and PID control. The fuzzy control was the easiest to implement and calibrate but in its implemented form was poor in performance.

This paper presents an early stage investigation into ABS systems for heavy vehicles. Chapter 2 presents a programme of field tests on an instrumented vehicle, chapter 3 develops a mathematical model of the vehicle and chapter 5 compares the measurements with simulation results. Finally chapter 6 presents an early investigation of wheel-slip control for heavy vehicles.

## FIELD TESTS

### Brake system modifications
Braking tests were performed on the tractor / semi-trailer combination shown in Figure 1. In order to investigate the performance of the trailer ABS system, the brakes on the tractor unit were disabled during the tests.



Figure 1. Tractor and semi-trailer combination used for testing.

A simple pneumatic circuit that could apply a constant brake pressure to the trailer brakes was developed (Figure 2) and inserted on the truck just upstream of the tractor/trailer coupling.

This circuit enabled the brake-pressure signal to be adjusted using the regulator prior to the test run. This pre-selected pressure was then applied down the service line of the trailer by the solenoid valve, using a switching signal generated by the operator in the tractor cab. The two-way valve is a safety measure that ensures that the driver an override the test-brake pressure by use of the normal foot-brake pedal or the handbrake, if required.
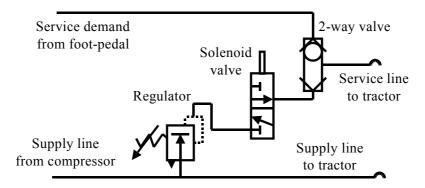
Figure 2. Modifications to brake pneumatics

## Instrumentation and data logging

The instrumentation used on the test vehicle is illustrated in figure 3. Two ICON's (industrial computers from Mektronika Systems, specifically designed for data logging and control) were used for logging the test data. One was located on the tractor and the other on the trailer. The ICON's logged at 250 Hz and low pass filters were set at 35 Hz. The ICON's communicated via CAN (Control Area Network) with a 'Global Controller' computer, which was located in the tractor.
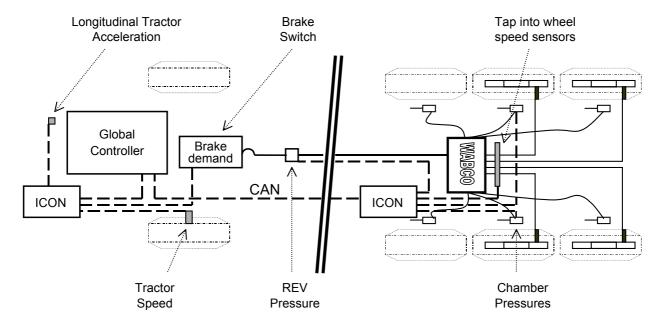


Figure 3. Tractor and trailer instrumentation.

The tractor ICON logged:
- The speed and longitudinal acceleration of the tractor.
- A voltage signal recording the switch time of the pressure solenoid valve that initiated braking.

The trailer ICON logged:
- The pressure at the Relay Emergency Valve (REV) at the front of the trailer. The pneumatic brake signal is converted into a CAN signal and sent to the ECU from the REV.
- The left and right brake chamber pressures on the second axle of the trailer.
- The wheel speeds on the second and third axles of the trailer. The wheel speed measuring instrumentation tapped into the voltages generated by the ABS wheel speed measurement transducers.

## Testing procedure

In each test, the driver took the vehicle out of gear a short time before the trailer brakes were engaged, the test engineer initiated the data-logger, so that a short period of coasting could be recorded, and then the braking solenoid was activated.

Three surfaces were used for testing:

- basalt tiles – nominal coefficient of friction of 0.2,
- 'bridport' – nominal coefficient of friction of 0.4, and
- 'delugrip' – nominal coefficient of friction of 0.75.

Three repeat tests were completed at nominal set brake pressures of 3 bar, 5 bar, and 8 bar on each of these surfaces.

It was at first desired that the tests would be conducted from an initial speed of 18 m/s (40 mph). This was so that the trailer brakes would dissipate approximately the same amount of energy as they would under normal operation, with all the brakes operating, when stopping from 27 m/s (60 mph). However, the straight line wet grip facility used for testing was too short to stop the tractor trailer combination from this speed, so the initial speed was reduced to 12 m/s (28 mph).

## MATHEMATICAL MODELLING

### Overall model

The mathematical model of the vehicle had four degrees of freedom: longitudinal motion of the whole vehicle (both tractor and trailer) and rotational motion of the wheels on each of the three trailer axles, as shown in Figure 4. The effects of aerodynamic inputs (e.g. wind disturbances, drag), road inputs (e.g. gradients and bumps), yaw, roll and bouncing motions of the vehicle as well as the vertical motion of the unsprung masses were neglected. Longitudinal load transfer due to quasi-static forward pitching motion of the trailer was included, but pitching dynamics were neglected.
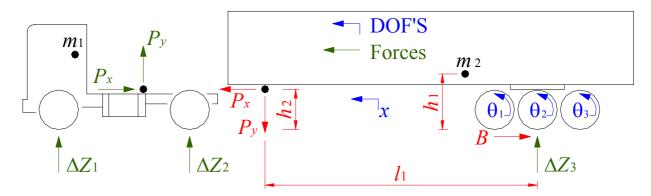


Figure 4. Heavy vehicle model.

Taking moments about the fifth wheel P:

$$\Delta Z_3 = \frac{-B(m_1 h_2 + m_2 h_1)}{l_1(m_1 + m_2)}$$

(1)

where $\Delta Z_3$ = resultant load transfer on all three rear axles,
B = the braking force on the trailer determined from the μ-λ slip curve,
$m_1$ = the mass of the tractor,
$m_2$ = the mass of the trailer,
$h_1$ = the trailer CoG height,
$h_2$ = the tow hitch height, and
$l_1$ = the wheel-base of the trailer.

The test trailer is 16 m long and relatively flexible. Consequently, the pitching moment on the trailer together with the compliance of the trailer chassis and suspension results in the normal load being transferred from the third axle, $Z_{33}$, to the first axle, $Z_{31}$ as shown in Figure 5.
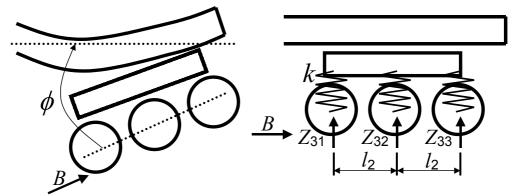
Figure 5. Chassis compliance.

A given braking force on the trailer B, will result in a specified deflection, $\phi$, in the chassis. This determines the proportioning of load on each axle:

$$\Delta Z_{31} = \frac{\Delta Z_3}{3} + \phi k l_2 \qquad (2)$$

$$\Delta Z_{32} = \frac{\Delta Z_3}{3} \qquad (3)$$

$$\Delta Z_{33} = \frac{\Delta Z_3}{3} - \phi k l_2 \qquad (4)$$

where  $\Delta Z_{3i}$  = the load transfer on the $i_{th}$ trailer axle,
   $\Delta Z_3$  = resultant load transfer on all three rear axles,
   $\phi$  = the chassis deflection,
   k  = equivalent spring stiffness of the trailer suspension,
   $l_2$  = distance between the suspensions springs.

Since the exact compliance, chassis stiffness and slop were unknown, a linear relationship was assumed between the braking force B and the chassis deflection $\phi$.

**ABS mechanics**
Figure 6 illustrates the mechanics of a typical heavy vehicle ABS system. The forces and moments on the braked wheel are illustrated in the top left corner, below which is the tyre force versus slip relationship ($\mu$-$\lambda$) plotted with the road friction moment $R_r B$ on the y-axis. On the right: the top graph shows the vehicle speed, $V_{vehicle}$, and wheel speed, $R_r \dot{\theta}$ for a typical brake actuation cycle; the middle graph shows the corresponding wheel acceleration, $R_r \ddot{\theta}$ and the bottom graph shows the corresponding brake torque, T.

Taking moments about the axle:

$$R_r B - T - \ddot{\theta} J = 0 \qquad (5)$$

where  $R_r$  = the rolling radius of the tyre,
   B  = the braking frictional force applied to the tyre by the road,
   T  = the braking torque,
   $\ddot{\theta}$  = the angular acceleration of the wheel, and
   J  = the moment of inertia of the wheel.

Equation 5 can be rearranged into:

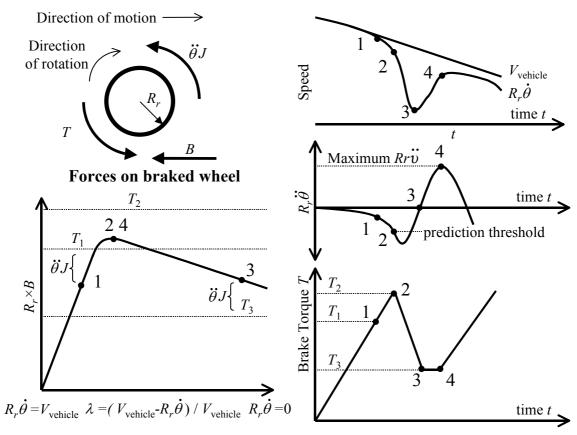$$\ddot{\theta}J = R_r B - T \qquad (6)$$



Figure 6. ABS mechanics.

From equation 6 the sign of the angular acceleration is negative at point 1. The braking torque $T_1$ is greater than the frictional force term $R_r B$. Consequently there is a decrease in the wheel speed and a shift to the right on the $\mu$-$\lambda$ slip curve. This results in an increase in $R_r B$ (braking of the truck) and a stable decrease in the angular deceleration.

If the braking torque is increased above the $\mu$-$\lambda$ slip curve, the system becomes unstable. At point 2, the angular deceleration increases rapidly and this further shifts the point on the $\mu$-$\lambda$ slip curve to the right. Wheel lock up is now imminent. This rapid decrease in the angular speed of the wheel is detected by the ABS algorithm and is known as the 'prediction' threshold. Once the 'prediction' threshold is reached, the ABS reduces the brake chamber pressure, reducing the brake torque to a lower value $T_3$. From equation 6 the sign of the angular acceleration then becomes positive at point 3. This drives the operating point on the $\mu$-$\lambda$ slip curve to the left. The angular acceleration first increases and then decreases back once the stable part of the $\mu$-$\lambda$ slip curve is reached. The acceleration having reached a maximum at point 4 is used as the 'reselection' criteria, the brake torque is increased, and the cycle continues.

Manufacturers' implementation of ABS is proprietary information, and thus the 'prediction' threshold and 'reselection' criteria are unknown and need to be back-engineered. By fitting exponential curves to experimentally measured brake chamber pressures (see Figure 7), the ABS logic of a Wabco 841 700 890 0 has been estimated. At each start of a new exponential curve the wheel velocities and accelerations were analysed to determine the logic that caused this change. The estimated ABS logic is given in Table 1.

Table 1. Estimated Wabco 841 700 890 0 ABS logic.

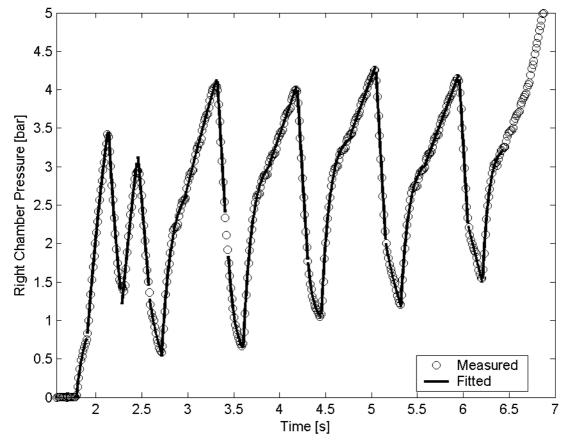| PREDICTION THRESHOLD | Reselection criteria | Further characteristics |
|---|---|---|
| $\ddot{\theta} = -2.3g$ | $\ddot{\theta} = \max$ | 0.3 bar pulsed pressure increase at t = 0.05 s after "reselection" |



Figure 7. Fitted curves right brake chamber, $\mu = 0.75$, P = 8 bar.

## Tyre modelling

Braking forces were calculated using the generic truck force data measured by UMTRI. (Fancher 1995). These results were modified using Pacejka's similarity method (Pacejka 2002) to adapt the braking curves to the required vertical load and coefficient of friction.

The similarity method is based on:
- the observation that the pure slip curves remain approximately similar in shape when the tyre runs at conditions that are different from the reference condition, and
- insight gained from the brush models.

A demonstration that similarity indeed approximately occurs is given by Radt and Milliken. (Radt 1983)

## Pneumatic lag modelling

The model of the brake signal is illustrated in Figure 8. Each first-order time lag contains a delay term and a time constant term, see Figure 9. With the EBS active the CAN delay $d_{2a}$ is considered to be negligible, and the time constant, $\tau_{2a}$ is set to zero. The experimental set-up illustrated in Figure 10 was used to determine the pneumatic time delays and time constants, on the test vehicle. The results are illustrated in  Figure 11 and Figure 12.

Results are given for both apply brake and release-brake signals, and the error bars show one standard deviation. As the pressure increases so the time delays decrease, but only slightly due to choking of the pneumatic pipes. The pneumatic signal cannot travel any quicker than the speed of sound in air. The time delays of the brake apply and brake release signals are very similar. Since the values of the time delays and time constants are not significantly dependent on the set brake pressures applied or if the brake is being applied or released, these values were averaged to calculate a single value. This considerably simplifies the simulation of the braking process. The averaged values are given in Table . The time constant $\tau_1 = 0.410$ s is comparatively large, and is assumed to be a result of the small bore of the ¼" BSP connection of the solenoid valve. Normal braking using the treadle valve of the foot pedal would probably have a faster response time.
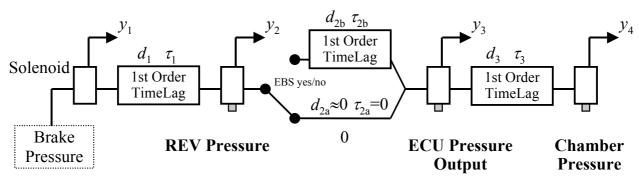


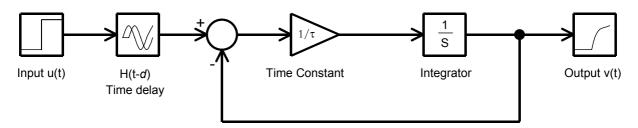Figure 8. Model of brake signal flow.
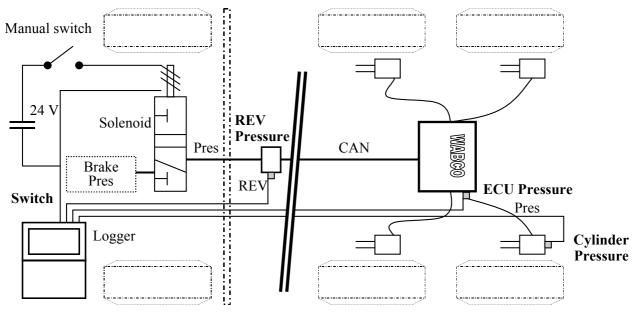


Figure 9. First-order time lag element.

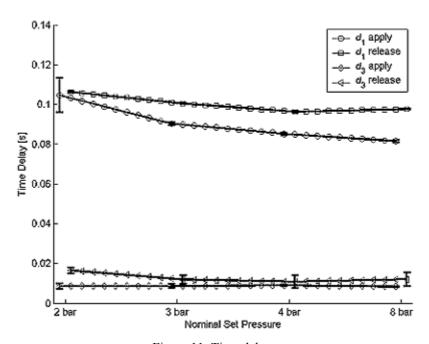

Figure 10. Experimental set-up to determine brake delays.
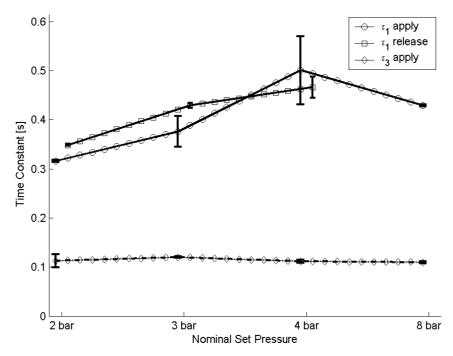
Figure 11. Time delays.



Figure 12. Time constants.

Table 2. Average measured time delays and time constants.

| $d_1$ [s] | $d_3$ [s] | $\tau_1$ [s] | $\tau_3$ [s] |
|---|---|---|---|
| 0.095 | 0.011 | 0.410 | 0.114 |

When simulating the performance of the ABS, it is $d_3$ and $\tau_3$ that are most important. These determine the delay of the ABS logic commands to the brake chambers and strongly influence the response speed of the system. Table 3 gives values measured by the University of Michigan Transport Research Institute (UMTRI) (Winkler 1992) for a number of other ABS systems. The time delays measured for the Wabco system are slightly smaller than the UMTRI values and the time constants are slightly larger. Furthermore, the UMTRI measurements show a significant difference between the apply-brake time constant and the release-brake time constant.

Table 3. Time delays and time constants as measured by UMTRI, (Winkler 1992).

| ABS System | $d_3$ apply [s] | $d_3$ release [s] | $\tau_3$ apply [s] | $\tau_3$ release [s] |
|---|---|---|---|---|
| Bendix | 0.025 | 0.025 | 0.11 | 0.045 |
| Kelsey-Hayes | 0.025 | 0.04 | 0.11 | 0.04 |
| B.F. Goodrich | 0.025 | 0.025 | 0.11 | 0.035 |
| Eaton | 0.03 | 0.03 | 0.11 | 0.04 |
| Wagner | 0.03 | 0.02 | 0.11 | 0.04 |

## Brake modelling

The brake model used is similar to that of Hardy and Cebon (Hardy 1993). The model neglects the effects of wheel speed, temperature and loading history. Post et al (Post 1975) tested brakes to find the relationship between chamber pressure and applied torque. Their results showed that the torque was approximately proportional to the pressure, with a proportionality constant, A, of 2.5 kNm/bar for S-cam brakes. Hysteresis was also present in the test data, particularly for S-cam brakes. This characteristic was included in the brake model by adding or subtracting a constant friction torque to the pressure component, depending on whether the total torque was increasing or decreasing. The total brake torque is given by:

$$T = AP_{\mathrm{cham}} \pm T_f \tag{7}$$

where
$T$ = the braking torque,
$A$ = a proportionality constant,
$P_{\mathrm{cham}}$ = the chamber pressure, and
$T_f$ = the hysteresis friction torque estimated from Post to be 200 Nm.

## Comparison of simulation and experimental results

The simulation and experimental results for braking on basalt ($\mu = 0.2$, and brake demand = 3 bar) and on 'delugrip' ($\mu = 0.75$ and brake demand = 8 bar) are shown in Figure 13 and Figure 14. The results show good agreement. Further improvements could be made by modifying the tyre model to account for the variation of maximum friction with speed. This is clearly evident from the experimental deceleration trace which increases as the vehicle nears the stop. Nevertheless the simulation is thought to be accurate enough for investigating the main behaviour of ABS systems.
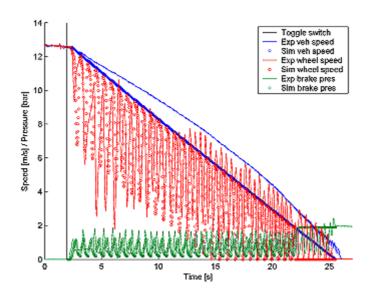


Figure 13. Comparison of simulation and experimental results $\mu$=0.2 brake demand = 3 bar.
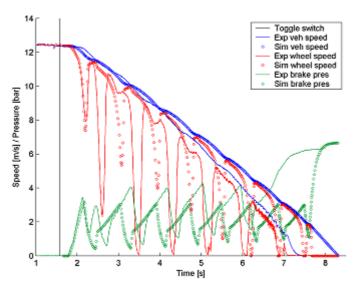
Figure 14. Comparison of simulation and experimental results μ=0.75 brake demand = 8 bar.

## SIMULATED WHEEL-SLIP CONTROL

In theory, an alternative approach to the 'bang-bang' control of conventional heavy vehicle ABS is wheel-slip control.

Figure 15 illustrates the model developed for implementing wheel-slip control on each axle of the semi-trailer. On each axle a brake-valve controller controls the brake pressure to the minimum of either the brake demand from the driver or the pressure set by the wheel-slip controller. Each wheel-slip controller is in turn controlled by the global controller, $K_{tot}$. The multiple-input, multiple-output (MIMO) control problem is further complicated by the saturation of the brake pressure actuation at 0 and 8 bar and by the non-linear tyre characteristics. In order to speed up the simulation runs when assessing the improvement of wheel-slip control, the pressure demand was assumed to be a step input. This does not directly effect the braking algorithm.
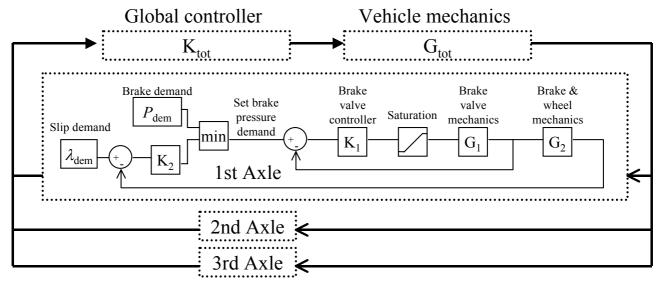


Figure 15. Implementation of wheel-slip control.

Figure 16 compares the braking distance of the conventional ABS technology to a preliminary wheel-slip controller. The wheel-slip controller was tuned using a trial and error technique for choosing the gains for the controllers $K_1$ and $K_2$. The results indicate that wheel-slip control has the potential to reduce the braking

distance by 25%. The figure also shows results that could be achieved if the hardware of the brake-valve controller could be improved to eliminate the lag $d_3$, and reduce the time constant to $\tau_3=0.02$ s.

A detailed analysis of the simulation output revealed that with the normal time delays and time constants, the controller saturated the brake-valve controller which cycled through fully open to fully closed at a frequency of about 3 Hz. This would be unacceptable in practice, since it would drain the air-supply reservoirs. However for the case when the valve-controller delays were improved, the wild overshoots in the valve controller were eliminated.

The model presented here assumed that slip under braking could be measured. This is not necessarily the case because the true vehicle speed is unknown once braking is initiated. Consequently, predicting wheel slip requires an accurate ground speed sensor or inference from other vehicle states, such as acceleration measurements. The feasibility of such instrumentation to implement practical wheel-slip control will be the subject of future research.



Figure 16. Performance improvement of wheel-slip control.

## CONCLUSIONS AND FURTHER WORK

- A mathematical model of the braking performance of an experimental vehicle has been developed. The model includes the details of vehicle dynamics, the ABS control algorithm as well as the mechanics of the foundation brakes and the pneumatic and mechanical systems.
- Parameters for the model were determined from tests on an instrumented experimental tractor semi-trailer.
- The vehicle braking model was validated by comparing its performance with tests on an instrumented heavy vehicle. Agreement between simulation and experiment was good.
- An initial study showed that there is potential to increase the braking performance of heavy vehicles using wheel-slip control, but improvement of the brake actuation system is required to maximise the performance.
- Further work is required to implement a suitable algorithm to handle the MIMO problem and to measure the true vehicle speed under braking.

## ACKNOWLEDGEMENTS

At the time of writing, the Cambridge Vehicle Dynamics Consortium has the following industrial members: Tinsley Bridge Ltd, ArvinMeritor, Koni BV, Qinetiq, Shell UK Ltd, Volvo Global Trucks, Crane Fruehauf, Firestone Industrial Products, Haldex Brake Products, MIRA Limited, Mektronika Systems and Fluid Power Design.

## REFERENCES

1. Akey, M. (1995). "Development of Fuzzy Logic ABS Control for Commercial Trucks." *SAE* 952673: 780788.
2. Akey, M. (1996). *Fuzzy logic ABS control: sizing theory to implementation*. Proceedings of SPIE - The International Society for Optical Engineering, Orlando.
3. Chen, F.-W., and Liao, T.-L. (2000). "Nonlinear Linearization Controller and Genetic Algorithm-based Fuzzy Logic Controller for ABS systems and their Comparison." *International Journal of Vehicle Design* 24(4): 334-349.
4. Fancher, P. S., and Macadam, C.C. (1976). "Computer Analysis of Antilock System Performance in the Braking of Commercial Vehicles." *IMechE* C32/76: 113-123.
5. Fancher, P. S. (1985). Integrating Anti-Lock Braking Systems with the Directional Control Properties of Heavy Trucks. Anti-Lock Braking Systems for Road Vehicles, London, IMechE.
6. Fancher, P. S. (1995). Generic Data for Representing Truck Tire Characteristics in Simulations of a Braking and Braking-in-a-Turn Maneuvers, University of Michigan Transport Research Institute UMTRI: 1-100.
7. Gissinger, G. L., Menard, C., Constans, A. (2003). "A Mechatronic Conception of a New Intelligent Braking System." *Control Engineering Practice* 11: 163-170.
8. Hardy, M. S., and Cebon, D. (1993). "Influence of Heavy Vehicle Suspensions on ABS Performance." SAE 932990: 109-116.
9. Hardy, M. S., and Cebon, D. (1995). "An Investigation of Anti-lock Braking Strategies for Heavy Goods Vehicles." *J. Auto. Eng., IMechE* 209(D4): 263-271.
10. Jun, C. (1998). *The Study of ABS Control System with Different Control Methods*. 4th International Symposium on Advanced Vehicle Control, Nagoya, Japan.
11. Kimbrough, S. (1994). "A Computer Investigation of the Performance Potential of an Advanced Brake Controller." *SAE* 940836: 1074-1086.
12. Kimbrough, S. (1999). "A Topology for Vehicle Stability and Handling Enhancement Via Wheelslip Control." *Innovations in Vehicle Design and Development DE* 101: 115-124.
13. MacAdam, G. C. (1985). Computer Model Predictions of the Directional Response and Stability of Driver-vehicle Systems during Anti-skid Braking. Anti-Lock Braking Systems for Road Vehicles, London, IMechE.
14. McLoughlin, J. H. (1985). *Limited Slip Braking*. Anti-Lock Braking Systems for Road Vehicles, London, IMechE.
15. Pacejka, H. A. (2002). *Tyre and Vehicle Dynamics*, Butterworth-Heinemann.
16. Palkovics, L., and Fries, A. (2001). "Intelligent Electronic Systems in Commercial Vehicles for Enhanced Traffic Safety." *Vehicle System Dynamics* 35(4-5): 227-289.
17. Post, T. M., Fancher, P.S., and Bernard, J.E. (1975). "Torque Characteristics of Commercial Vehicle Brakes." SAE.
18. Radt, H. S., and Millken, W.F. (1983). *Non-Dimensionalizing Tyre Data for Vehicle Simulation*. Road Vehicle Handling, Nuneaton, IMechE.
19. Will, A. B., and Zak, S.H. (2000). "Antilock Brake System Modelling and Fuzzy Control." *International Journal of Vehicle Design* 24(1): 1-18.
20. Winkler, C. B. (1992). The Mechanics of Heavy Vehicles, Course Notes. Wolfson College Cambridge.
21. Yu, F., Feng, J.-Z., and Li, J. (2002). "A Fuzzy Logic Controller Design for Vehicle ABS with a On-Line Optimised Target Wheel Slip Ratio." *International Journal of Automotive Technology* 3(4): 165-170.
22. Zanten, A. T. v. (2002). *Evolution of Electronic Control Systems for Improving the Vehicle Dynamic Behavior*. 6th International Symposium on Advanced Vehicle Control, AVEC '02, Hiroshima, Society of Automotive Engineers of Japan, Inc.